Remote Sensing of Environment 112 (2008) 3055-3063

Contents lists available at ScienceDirect

Remote Sensing of Environment

journal homepage: www.elsevier.com/locate/rse

Active fire detection and characterization with the advanced spaceborne thermal emission and reflection radiometer (ASTER)

Louis Giglio [a,b,*], Ivan Csiszar [b], Ágoston Restás [c], Jeffrey T. Morisette [d], Wilfrid Schroeder [b], Douglas Morton [b], Christopher O. Justice [b]

[a] Science Systems and Applications, Inc., Lanham, Maryland, USA
[b] Department of Geography, University of Maryland, College Park, Maryland, USA
[c] Szendrő Fire Department, Szendrő, Hungary
[d] NASA Goddard Space Flight Center, Greenbelt, Maryland, USA

ARTICLE INFO

Article history:
Received 16 October 2007
Received in revised form 26 February 2008
Accepted 1 March 2008

Keywords:
Biomass burning
Fire detection
Fire radiative power
ASTER
MODIS

ABSTRACT

We present an automated fire detection algorithm for the Advanced Spaceborne Thermal Emission and Reflection Radiometer (ASTER) sensor capable of mapping actively burning fires at 30-m spatial resolution. For daytime scenes, our approach uses near infrared and short-wave infrared reflectance imagery. For nighttime scenes a simple short wave infrared radiance threshold is applied. Based on a statistical analysis of 100 ASTER scenes, we established omission and commission error rates for nine different regions. In most regions the probability of detection was between 0.8 and 0.9. Probabilities of false alarm varied between 9×10^{-8} (India) and 2×10^{-5} (USA/Canada). In most cases, the majority of false fire pixels were linked to clusters of true fire pixels, suggesting that most false fire pixels occur along ambiguous fire boundaries. We next consider fire characterization, and formulate an empirical method for estimating fire radiative power (FRP), a measure of fire intensity, using three ASTER thermal infrared channels. We performed a preliminary evaluation of our retrieval approach using four prescribed fires which were active at the time of the Terra overpass for which limited ground-truth data were collected. Retrieved FRP was accurate to within 20%, with the exception of one fire partially obscured by heavy soot.

1. Introduction

At present a number of satellite-based active fire, or "hot spot", data products are available for operational and experimental use. The number of sensors from which these data sets are derived has grown considerably over the past decade, and now includes the Advanced Very High Resolution Radiometer (AVHRR), the Moderate Resolution Imaging Spectroradiometer (MODIS), the Along-Track Scanning Radiometer (ATSR) and Advanced Along-Track Scanning Radiometer (AATSR), the Visible and Infrared Scanner (VIRS), the Geostationary Operational Environmental Satellite (GOES) Imager, the Operational Linescan System (OLS), and the Spinning Enhanced Visible and Infrared Imager (SEVIRI) (Arino & Rosaz, 1999; Elvidge et al., 1996; Giglio et al., 2003; Justice et al., 1996, 2002; Prins et al., 2001; Roberts and Wooster, 2007; Stroppiana et al., 2000) While a variety of intercomparisons between satellite-based active fire data sets (or between the fire detection approach associated with each) have been performed (Li et al., 2001; Ichoku et al., 2003), there has been little rigorous product validation. The primary reason for this arises from the dynamic nature of fire and the short time scales over which it interacts with, and moves across, the landscape. Continued interest exists, therefore, in using high resolution sensors on board aircraft or satellites to provide spatially and temporally coincident fire imagery. The resulting fire "snapshots" could then be used to derive detailed, instantaneous maps of fire extent (and perhaps properties) to support validation. In addition, high resolution fire maps are independently useful for ecological field studies on fire and its effects, especially in heterogeneous landscapes and at the wildland–urban interface.

A high-resolution sensor that has facilitated fire validation in recent years is the Advanced Spaceborne Thermal Emission and Reflection Radiometer (ASTER), a 14-channel imaging radiometer on board the National Aeronautics and Space Administration's (NASA) Terra satellite. Since ASTER co-resides with the Terra MODIS instrument, high resolution ASTER fire masks have become an important tool in the ongoing validation of the 1-km Terra MODIS active fire products initiated by Morisette et al. (2005a,b) and Csiszar et al. (2006). Since manual production of fire masks is time consuming, and simple fixed threshold methods do not scale well (both spatially and temporally), a consistent, automated source of ASTER fire masks is desirable. In this paper we present a fire detection algorithm that uses ASTER observations to provide binary "yes/no" fire masks at 30-m spatial resolution.

* Corresponding author. Science Systems and Applications, Inc., Lanham, Maryland, USA.
E-mail address: louis_giglio@ssaihq.com (L. Giglio).

0034-4257/$ – see front matter © 2008 Elsevier Inc. All rights reserved.
doi:10.1016/j.rse.2008.03.003

Table 1
ASTER channel characteristics

Band Number	Central Wavelength (μm)	Spatial Resolution
1	0.56	15 m
2	0.66	
3N	0.82	
3B	0.82	
4	1.65	30 m
5	2.17	
6	2.21	
7	2.26	
8	2.33	
9	2.40	
10	8.30	90 m
11	8.65	
12	9.10	
13	10.60	
14	11.30	

Algorithm performance is evaluated using 100 ASTER scenes for which fire pixels were manually identified. We next consider the potential of ASTER for fire characterization, and present an empirical method for retrieving fire radiative power (FRP), a measure of fire intensity, using ASTER data. The method is then evaluated using ground truth data obtained for several prescribed fires.

2. The ASTER instrument

The ASTER is a 14-channel imaging radiometer with separate visible and near-infrared (VNIR), short wave infrared (SWIR), and thermal infrared (TIR) optical subsystems (Yamaguchi et al., 1998). The individual subsystems contain four (VNIR), six (SWIR), and five (TIR) spectral bands at 15, 30, and 90 m spatial resolution, respectively. The ASTER band numbering and spectral locations are listed in Table 1. The VNIR and SWIR bands have three and four individually-selectable gain settings, respectively, referred to as *high*, *normal*, *low-1*, and *low-2* (SWIR only). The imaging swath for all bands spans 60 km. Due to various hardware, power, and data storage and download rate constraints, ASTER does not continuously acquire data, but is instead operated on a prioritized acquisition schedule (Yamaguchi et al., 1998).

3. Data

For this study we used 196 radiometrically calibrated and geometrically coregistered Level 1B ASTER scenes acquired between early 2001 and late 2004 for algorithm testing and evaluation. Scene locations and acquisition dates were selected based on current knowledge of the global distribution of fire activity. The locations of all scenes are shown in Fig. 1.

4. Fire detection

4.1. Band selection

Satellite-based fire detection has traditionally relied upon bands located near 4 μm to exploit the high levels of black-body radiation emitted at typical fire temperatures in this region of the electromagnetic spectrum. This region is, in fact, near-optimal for satellite-based fire detection in daytime imagery. This can be seen by considering the ratio R of black-body radiation emitted by a fire (L_{fire}) to the radiance of the ambient non-fire land surface (L_{land}):

$$R = L_{\text{fire}}/L_{\text{land}}. \tag{1}$$

The land radiance is composed of reflected solar radiation and thermal black-body radiation. For now we consider a simplified case of a Lambertian grey-body surface, unit fire emissivity, and no atmosphere. With the Sun located directly overhead, the ratio in Eq. (1) is given by

$$R(\lambda) = \frac{B(\lambda, T_{\text{fire}})}{\rho B(\lambda, T_{\text{sun}})\Omega_{\text{sun}}/\pi + (1-\rho)B(\lambda, T_{\text{land}})} \tag{2}$$

where $B(\lambda, T)$ is the Planck function, ρ is the land surface reflectance, T_{land} is the land surface temperature, and Ω_{sun} is the solid angle subtended by the Sun. The Planck function, which describes the spectral radiance emitted at wavelength λ by a black-body at temperature T, is given by

$$B(\lambda, T) = c_1\lambda^{-5}\left[\exp\left(\frac{c_2}{\lambda T}\right) - 1\right]^{-1} \tag{3}$$

where c_1 and c_2 are constants. In Fig. 2, the ratio $R(\lambda)$ is shown for representative flaming (~1000 K) and smoldering (~600 K) fires. Sensitivity peaks near 4 μm for both cases.

Among the most egregious of the simplifications we have made is the assumption of a grey body surface. In reality, of course, surface reflectance varies considerably with wavelength, and the constant ρ appearing in Eq. (2) should be replaced with the function $\rho(\lambda)$. If we were to substitute the reflectance spectrum of most natural terrestrial components into Eq. (2), the general shape of the curve in Fig. 2 would still resemble that of the ideal case, and peak sensitivity would remain near 4 μm. In contrast, including the atmosphere (which we have

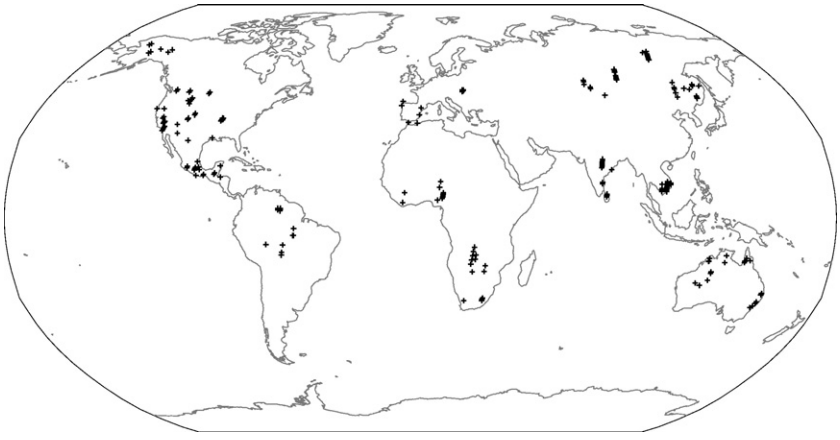

Fig. 1. Locations of the 196 ASTER scenes used in this study.